Mon. Not. R. Astron. Soc. **386,** 953–962 (2008) doi:10.1111/j.1365-2966.2008.13077.x

Exploring the infrared/radio correlation at high redshift

Edo Ibar,[1⋆] Michele Cirasuolo,[1] Rob Ivison,[1,2] Philip Best,[1] Ian Smail,[3] Andy Biggs,[2] Chris Simpson,[4] Jim Dunlop,[1] Omar Almaini,[5] Ross McLure,[1] Sebastien Foucaud[5] and Steve Rawlings[6]

[1]*Scottish Universities Physics Alliance, Institute for Astronomy, University of Edinburgh, Blackford Hill, Edinburgh EH9 3HJ*
[2]*UK Astronomy Technology Centre, Royal Observatory, Blackford Hill, Edinburgh EH9 3HJ*
[3]*Institute for Computational Cosmology, Durham University, South Road, Durham DH1 3LE*
[4]*Astrophysics Research Institute, Liverpool John Moores University, Twelve Quays House, Egerton Wharf, Birkenhead CH41 1LD*
[5]*School of Physics and Astronomy, University of Nottingham, University Park, Nottingham NG7 2RD*
[6]*Astrophysics, Department of Physics, Denys Wilkinson Building, Keble Road, Oxford OX1 3RH*

Accepted 2008 February 5. Received 2008 January 11; in original form 2007 October 9

ABSTRACT

We have analysed the 24-μm properties of a radio-selected sample in the Subaru–*XMM–Newton* Deep Field in order to explore the behaviour of the far-infrared/radio (FIR/radio) relation at high redshifts. Statistically, the correlation is described by q_{24}, the ratio between the observed flux densities at 24 μm and 1.4 GHz, respectively. Using 24-μm data results in considerably more scatter in the correlation than previous work using data at 60–70 μm. Nevertheless, we do observe a steady correlation as a function of redshift, up to $z \approx 3.5$, suggesting its validity back to primeval times. We find $q_{24} = 0.30 \pm 0.56$ for the observed and $q_{24} = 0.71 \pm 0.47$ for the *k*-corrected radio sample, based on sources with 300 μJy $< S_{1.4\,\mathrm{GHz}} <$ 3.2 mJy and 24-μm detections. A suitable *k*-correction given by a M82-like mid-infrared (mid-IR) template suggests no extreme silicate absorption in the bulk of our radio sample. Using thresholds in q_{24} to identify radio-excess sources, we have been able to characterize the transition from radio-loud active galactic nuclei (AGN) to star-forming galaxies and radio-quiet AGN at faint ($\lesssim$1 mJy) radio-flux densities. Our results are in broad agreement with previous studies which show a dominant radio-loud AGN population at >1 mJy. The rest-frame $U - B$ colours of the expected radio-excess population have a redder distribution than those that follow the correlation. This is therefore a promising way to select obscured type 2 AGN, with a radio-loud nature, missed by deep X-ray observations. Spectroscopic follow-up of these sources is required to fully test this method.

Key words: galaxies: active – galaxies: fundamental parameters – galaxies: high-redshift – galaxies: starburst.

1 INTRODUCTION

The far-infrared/radio (FIR/radio) relation is one of the tightest correlations known in astronomy. Established over the three decades ago (e.g. van der Kruit 1971; Helou, Soifer & Rowan-Robinson 1985), it covers about five orders of magnitude in luminosity (Condon 1992; Garrett 2002). The correlation is tightest for local star-forming galaxies and relates the integrated thermal emission, from the dust present in star-forming regions, with the non-thermal synchrotron emission produced by relativistic particles (cosmic rays) accelerated by supernovae explosions (Harwit & Pacini 1975). A complete explanation of the origin of this remarkable correlation is essential for our understanding of how galaxies formed and evolved, particularly if the correlation extends from primeval galaxies to the fully mature galaxies observed locally, as recent studies have hinted (Kovács et al. 2006).

Being relatively direct probes of recent star formation, FIR and radio data are amongst the most powerful tools available to test whether primordial galaxies shared the same properties as galaxies present today. Low-frequency radio data have been used to estimate redshifts using radio-to-submm flux density ratios (e.g. Carilli & Yun 2000), and to determine the cosmic star-formation history (e.g. Haarsma et al. 2000; Ivison et al. 2007a), facilitating the investigation of the cosmic infrared (IR) background (CIRB). If the relation between flux densities observed in the FIR and radio wavebands holds at high redshifts, then we can exploit ultra-deep high-resolution radio imaging to resolve the CIRB and to explore the properties of luminous distant galaxies – for example, studies of submm galaxies (Smail, Ivison & Blain 1997; Hughes et al. 1998)

⋆E-mail: ibar@roe.ac.uk

which are encumbered by the confusion encountered in the submm (rest-frame FIR) waveband, and studies of active galactic nuclei (AGN; Beelen et al. 2006) that are subject to selection biases caused by obscuration at shorter wavelengths.

While the combination of *Spitzer* observations at 24 and 70 μm and radio observations at 1.4 GHz support the universality of the FIR/radio correlation up to a redshift of approximately unity (Appleton et al. 2004), extending this correlation to higher redshifts requires extremely deep and complementary observations at radio and IR wavelengths, as well as reliable estimates of redshift. The work presented here is based on a deep multi-wavelength study in the Subaru–*XMM–Newton* Deep Field (SXDF). We have exploited 1.4-GHz images from the Very Large Array (VLA), reaching a 5σ flux density threshold of ~ 35 μJy and covering an area of approximately 1 deg^2. The region has also been observed to impressive depths at optical (SuprimeCAM; Furusawa et al. in preparation), near-IR (UKIDSS-UDS; Lawrence et al. 2007) and mid-IR (*Spitzer* Wide-area IR Extragalactic Survey – SWIRE; Lonsdale et al. 2003) wavelengths.

Starburst galaxies, radio-quiet AGN and radio-loud AGN are the three main populations which can be observed to high redshifts with the data employed in this work. It is known that radio-quiet AGN (i.e. Seyfert galaxies) follow the FIR/radio correlation (Roy et al. 1998), but radio-loud AGN may vary considerably in radio luminosities due to their extra core and jet radio emission, thus weakening and biasing the correlation. In theory, it is possible to identify these radio-loud AGN via their deviation from the expected relation and therefore to determine the fraction of these so-called 'radio-excess' sources as a function of radio-flux density. This would then allow us to constrain the predictions of synthesis population models for the transition at submJy radio fluxes from radio-loud AGN to starburst/radio-quiet AGN (Dunlop & Peacock 1990; Jarvis & Rawlings 2004).

The aim of this work is to explore and discuss the correlation between the monochromatic fluxes at 24 μm and 1.4 GHz across a broad range of redshifts, and test the capabilities of the relation for selecting radio-loud AGN (e.g. Donley et al. 2004).

In Section 2, we present the multi-wavelength data available for the SXDF field and used in this work. Section 3 shows the capabilities of the data to extend the 24 μm/1.4 GHz correlation to higher redshifts, and Section 4 describes the process of detecting radio-loud AGN at submJy 1.4-GHz flux densities. The discussion and conclusions are presented in Sections 5 and 6, respectively. Throughout this paper, we have used $\Omega_{\rm m} = 0.3$, $\Omega_\Lambda = 0.7$ and $H_0 = 70$ km s^{-1} Mpc^{-1} (Spergel et al. 2007).

2 SXDF OBSERVATIONS

2.1 Radio observations at 1.4 GHz

Radio observations of the SXDF were carried out by Ivison et al. (2007b) during 2003 July using the VLA at 1.4 GHz. The total integration time was approximately 60 h, reaching an rms depth of 7 μJy beam^{-1} near the centre of the field. The radio map is centred at RA 2$^{\rm h}$18$^{\rm m}$, Dec. -5° 0′, with a synthesised beam of 1.86 × 1.61 arcsec^2 at position angle 15°. The source detection was carried out using a 5σ threshold, sufficient to avoid significant contamination by spurious sources, obtaining a total number of 563 radio sources in an area of $\sim$0.45 deg^2.

In order to exploit the larger area covered by previous multi-wavelength observations in the SXDF, we have also used the 1.4-GHz catalogue presented by Simpson et al. (2006). Their observations comprised 13 VLA pointings reaching a mosaic rms noise of $\sim$12–20 μJy beam^{-1}. The Simpson et al. catalogue contains 505 sources and covers 0.8 deg^2 to a flux-density limit of 100 μJy.

By combining both radio samples, we obtained a total sample of 828 radio sources. Extended sources and obvious doubles, identified by eye, were considered as single emitters. The distribution of radio-flux densities peaks at about 100 μJy and reaches flux densities as faint as 35 μJy (5σ) and as bright as 80 mJy.

2.2 *Spitzer* observations

The SXDF was observed by *Spitzer* as part of the SWIRE Legacy programme. The SXDF is included in one of the seven high-latitude SWIRE fields, the *XMM*–LSS field, with coverage of 9.1 deg^2. Observations were obtained at 3.6, 4.5, 5.8 and 8.0 μm with *IRAC* and at 24, 70 and 160 μm with Multiband Imaging Photometer for *Spitzer* (MIPS; Surace et al. 2005). In order to explore the FIR/radio correlation, we have used only the detections at 24 μm. It is known that use of the monochromatic 24-μm flux densities yields a larger scatter than the 70-μm data (Appleton et al. 2004); however, we are limited by the relatively shallow coverage at 70 μm and the more severe confusion at that wavelength.

To explore the FIR/radio relation as a function of redshift, we use the combined radio source catalogue described in Section 2.1 to cross-match it with the conservative (10σ) SWIRE source catalogue retrieved from the *Spitzer* Centre Archive. We obtained 370 counterparts with fluxes $S_{24\,\mu{\rm m}} \gtrsim 0.4$ mJy using a 12.5-arcsec-diameter aperture for the photometry.

We then extended the catalogue to fainter 24-μm flux densities by measuring the observed flux density on the 24-μm map, using the same diameter aperture centred at the radio positions. This allowed the inclusion of 125 sources with 24-μm flux densities of $S_{24\,\mu{\rm m}} \gtrsim 200$ μJy ($\sim 4\sigma$; Shupe et al. 2008). In this paper, for all the remaining radio sources we used upper limits at $S_{24\,\mu{\rm m}} = 200$ μJy.

2.3 Subaru and UKIRT observations

The SXDF is home to the very deep optical survey undertaken by Subaru/SuprimeCAM (Miyazaki et al. 2002). This comprises five overlapping pointings, providing broad-band photometry in the $BVRi'z'$ filters to typical 5σ (*AB* magnitude) depths of $B = 27.5$, $V = 26.7$, $R = 27.0$, $i' = 26.8$ and $z' = 25.9$, respectively (2-arcsec-diameter apertures). The seeing in the composite images is $\sim$0.8 arcsec (Sekiguki et al. 2005).

The central region of the SXDF is also being observed at near-IR wavelengths with the Wide-Field Camera (WFCAM) on the 3.8-m United Kingdom Infrared Telescope (UKIRT). As the deepest tier of the UKIRT Infrared Deep Sky Survey (UKIDSS, Lawrence et al. 2007), the Ultra Deep Survey (UDS) aims to cover 0.8 deg^2 to $K_{AB} = 25$. In this work, we use the UKIDSS First Data Release (DR1; Warren et al. 2007) where the 5σ point source depths (in *AB* magnitudes) at *J* and *K* are 23.61 and 23.55, with seeing of 0.86 and 0.76 arcsec, respectively.

We have used the *K*-band as the reference to cross-match with all other near-IR and optical images. Unfortunately, the UDS map misses part of the radio coverage of the SXDF field, limiting the radio sample to an area with 726 radio sources, of which 639 (88 per cent) have clear counterparts in the UDS *K* data within a search radius of 1.5 arcsec.

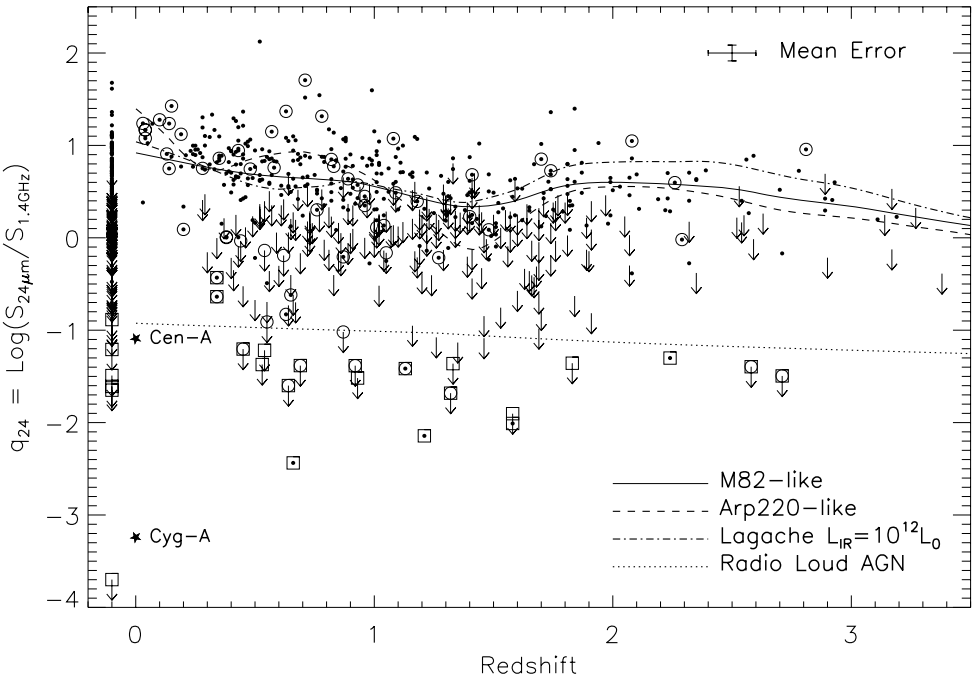

Figure 1. Black dots: ratio between the observed monochromatic fluxes at 1.4 GHz and 24 μm, $q_{24} = \log(S_{24\,\mu m}/S_{1.4\,GHz})$, as a function of redshift. Downward arrows: upper limits considering a mid-IR flux threshold given by 200 μJy. Note that these data have not been *k*-corrected. Sources without photo-*z*s are plotted at $z = -0.1$. Large circles: sources with spectroscopic redshifts. Large squares: sources with radio-flux densities $S_{1.4\,GHz} > 3.2$ mJy. Uncertainties in the observed flux densities give an average q_{24} mean error of ∼0.1 dex, and error bars in redshift are approximately $\sigma_z \approx 0.1$ (Cirasuolo et al. 2007). Overplotted lines show different *k*-correction factors, $K(24\,\mu m)/K(1.4\,GHz)$, for the observed q_{24} values as a function of redshift. The assumed mid-IR templates were convolved with the 24-μm filter from *Spitzer*/MIPS and are used to show the expected variation of the q_{24} values as a function of redshift. Three of these mid-IR templates are based on star-forming galaxies: two local standard massive starburst galaxies, M82 and Arp 220, and a SED model for an ULIRG galaxy with $L_{IR} = 10^{12}\,L_{\odot}$, as described by Lagache et al. (2004). All these three templates are assumed to have a simple spectral index $\alpha = -0.7$ for the radio emission, where $S_\nu \propto \nu^\alpha$, and normalized to the best fit to the data detections. Finally, a composite spectrum for radio-loud AGN given by Elvis et al. (1994) is also included, although as indicated by the locations of Cen-A and Cygnus-A, radio-loud AGN may be distributed over a wide range of q_{24} values. In particular, this template is not normalized to the best fit but uses values from the actual composite spectrum at both wavelengths.

2.4 Photometric redshifts

We obtained reliable photometric redshifts for 586 of the radio sources detected at near-IR wavebands. The estimation was carried out using all available detections from the *B*, *V*, *R*, *i*′, *z*′, *J*, *K*, 3.6- and 4.5-μm photometric bands and considering a conservative criteria: not including either those sources with poor χ^2 fitting nor those contaminated by haloes from nearby stars.

The spectral energy distribution (SED) fitting procedure provides a photometric estimation consistent within $\Delta z/(1+z) = 0.05 \pm 0.04$ for the UDS galaxies in general (see Cirasuolo et al. 2007, for details), and spectroscopic redshifts available for 63 of the 586 radio sources (Yamada et al. 2005; Simpson et al. 2006, and the NASA Extragalactic Data base) indicate that the photometric redshifts of the radio sources are also accurate at this level. The precision of this estimation is good enough to allow an adequate *k*-correction to the data (see Fig. 1). The resulting redshift distribution of the radio sources peaks at about $z \sim 0.7$ and includes galaxies up to $z \approx 3.5$.

Note that since the photometric redshift estimation depends on the *K*-band detection, the sample is basically mass limited. Dwarf galaxies with faint radio emission may be missed in the *K*-band, but massive ones are expected to be detected up to very high redshift. Heavily obscured galaxies, however, are not drastically affected.

3 THE FIR/RADIO RELATION

Based on the analysis presented in Section 2, 369 sources (out of potentially 726 due to the missed UDS area) have both a 24-μm detection with flux density $S_{24\,\mu m} > 200$ μJy and a reliable redshift (49 of which are spectroscopic).

We present in Fig. 1 the FIR/radio relation in terms of the basic observable parameter, q_{24} – the ratio between the monochromatic fluxes at 24 μm and 1.4 GHz, $\log(S_{24\,\mu m}/S_{1.4\,GHz})$ – as a function of redshift. Ideally, the correlation should be calculated using the bolometric FIR flux; however, the paucity of long-wavelength data makes this quantity difficult to estimate prior to the future arrival of Submillimetre Common-User Bolometer Array-2 (SCUBA-2) (Holland et al. 2006) and/or the *Herschel Space Observatory* (Poglitsch et al. 2006).

3.1 Non-*k*-corrected data

Fig. 1 shows that the vast majority of the sources detected at 24 μm follow a tight correlation between q_{24} and redshift, up to $z \approx 3.5$. Upper limits have been included using $S_{24\,\mu m} = 200$ μJy, and show probable evidence for a large number of radio-excess sources (i.e. radio-loud AGN) at the observed radio-flux density regime.

K-corrections to the data have been tested assuming standard starburst galaxy templates for the 24-μm detections and a

simple power slope for the radio density fluxes. The expected variations of q_{24} as a function of redshift are overplotted in Fig. 1, and are used to study and characterize the distribution for star-forming galaxies. Nevertheless, the presence of radio-loud AGN sources in the sample introduces outliers in the correlation that may cover a wide range of q_{24} values due to radio-excess emission coming from core and jet structures. For example, radio-loud AGN such as Cygnus A (a powerful double-lobed radio galaxy) and Centaurus A (one of the closest known radio galaxies) have $q_{24} = -3.2$ and -1.1 values, respectively, far from the main data trend from Fig. 1. In particular, our data show that the population with $S_{1.4\,\mathrm{GHz}} > 3.2$ mJy ($10^{-2.5}$ Jy; large squares in Fig. 1), characterized to be AGN-dominated by Condon (1992), have $q_{24} \lesssim -1$, well below the bulk of the data points and similar to the estimation obtained from a composite radio-loud AGN template (Elvis et al. 1994). Since we expect and want a correlation valid for star-forming systems, sources with $S_{1.4\,\mathrm{GHz}} > 3.2$ mJy are excluded from our analysis of the FIR/radio correlation, basically because these sources are radio-loud AGN that introduce biases in the statistics.

Using the biweight estimator[1] (Beers, Flynn & Gebhardt 1990) to characterize the data, we find a central location (mean) and scale parameter (σ; all q_{24} values quoted in this paper will similarly be given in this way) given by $q_{24} = 0.66 \pm 0.39$ (based on all detections at 24 μm including sources without estimated redshifts). The subsample of sources with $0 < z < 1$ gives an observed $q_{24} = 0.80 \pm 0.33$, in agreement with the results of Appleton et al. (2004), i.e. $q_{24} = 0.84 \pm 0.28$. The data also suggest a decreasing trend of q_{24} as a function of redshift. A simple linear regression to the 24-μm detected sources with estimated redshift gives a dependency $q_{24}(z) = (0.85 \pm 0.01) + (-0.20 \pm 0.01)\,z$. Nevertheless, this trend is probably seen because data have not been *k*-corrected (Hogg et al. 2002) as we described later. A summary of the various q_{24} values in this section is given in Table 1. It is worth noting that the available 49 sources with spectroscopic redshifts support the validity of the photometric estimation at high redshift (large circles in Fig. 1).

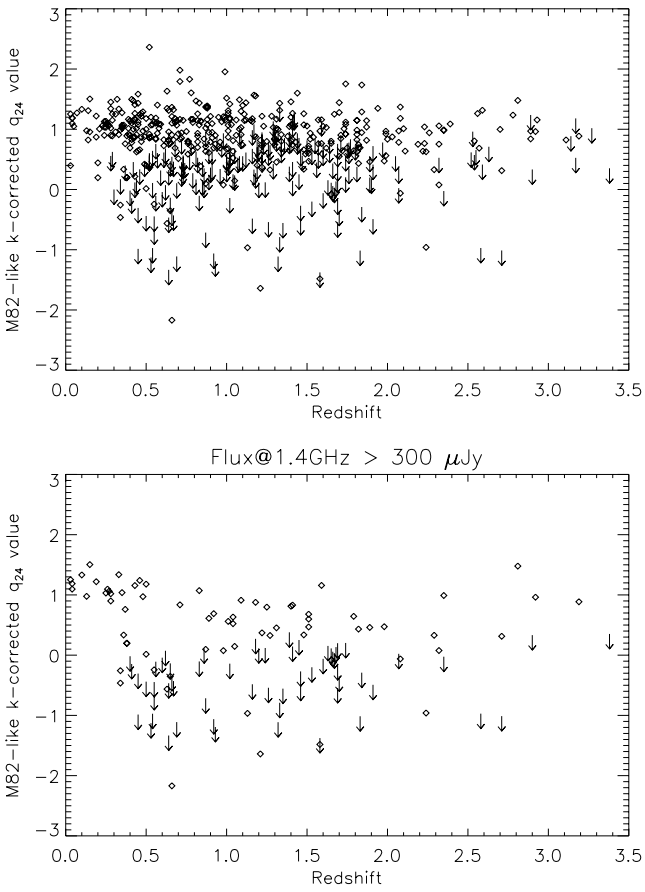

Figure 2. *K*-corrected q_{24} values as a function of redshift. The *k*-correction uses a M82-like template (Silva et al. 1998) for the mid-IR and a spectral slope $\alpha = -0.7$ for the radio emission ($S_\nu \propto \nu^\alpha$). Top panel: full radio sample. Bottom panel: radio sources with 1.4-GHz flux densities above 300 μJy. Upper limits are considered at $S_{24\,\mu\mathrm{m}} = 200$ μJy.

3.2 *k*-corrected data

IR spectroscopic studies of local starburst galaxies have shown three main components in the mid-IR range (5–38 μm): silicate bands around 10 and 18 μm, a large number of polycyclic aromatic hydrocarbon (PAH) emission features and a slope of the spectral continuum, where an AGN may be present (Brandl et al. 2006). In order to model the *k*-correction to the mid-IR emission from the bulk of the star-forming sources, we have convolved the SED of M82 (a local standard starburst galaxy with a distribution obtained from a fit to the observed photometry presented by Silva et al. 1998), Arp 220 (obtained from photometry listed in the NASA/IPAC Extragalactic Database and compiled by Pope et al. 2006) and a model of an ultraluminous IR galaxy (ULIRG; $L_{\mathrm{IR}} = 10^{12}\,\mathrm{L}_\odot$) given by Lagache et al. (2004), with the 24-μm filter profile from *Spitzer*/MIPS. The radio emission is assumed to be well represented by a power law with a spectral index $\alpha = -0.7$, based on an average steep-spectrum radio source (Condon 1992).

Note that assumptions of different mid-IR templates may largely change the q_{24} values at high redshift, mainly due to the 10-μm silicate feature redshifted to $z \approx 1.5$, where variations of even an order of magnitude in *k*-correction are seen. On the other hand, if we consider an extreme error in the radio spectral slope of $\sigma(\alpha) = 0.5$ (see findings in Garn et al. 2007), we find that the *k*-correction may change in ∼0.3 dex at $z \approx 3.5$, a value much lower than the 24-μm uncertainties.

The overplotted lines, in Fig. 1, show the expected change in the observed q_{24} parameter as a function of redshift based on the different adopted templates. Apart from the composite radio-loud spectra, the *k*-corrections have been normalized to the best fit to the data.

A descending trend in q_{24} as a function of redshift is expected from all three starburst-like *k*-corrections, in agreement with the observed slope. The *k*-corrected relation based on sources with mid-IR detections (>200 μJy) and estimated redshifts, changes to $q_{24} = 0.99 \pm 0.32$, 1.45 ± 0.38, and 1.08 ± 0.37 (biweight estimator) using the M82-like, Arp 220-like and the Lagache et al. model, respectively. The M82-like *k*-corrected q_{24} values are presented in the upper panel of Fig. 2 to demonstrate the improvement in the correlation as a function of redshift. Fig. 3 shows a redshift-binned version of this plot (for the 24-μm detected sources), demonstrating that both the mean and scatter of the M82-like *k*-corrected q_{24} value remain constant out to $z \sim 3.5$; it also demonstrates that *k*-correcting with an Arp220-like spectrum leads to large variations in the relation with redshift. Based upon the behaviour of the M82-like *k*-corrected distribution, and particularly the lack of a clear excess in scatter for

[1] In order to statistically describe the data, we used the biweight estimator which is resistant to outliers and is also robust for a broad range of non-Gaussian distributions. This is essential to remove the remaining AGN from the statistics of the sample.

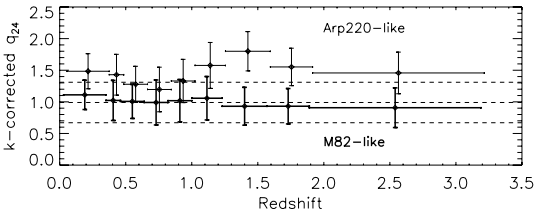

Figure 3. Binned mean and scatter of the M82-like *k*-corrected 24 μm/1.4 GHz correlation (thick black data) as a function of redshift, based on the full radio sample. The overplotted lines correspond to the mean and 1σ limits, for the all-redshift distribution. Also shown (in thin black data) are the equivalent values for an Arp220-like *k*-correction (shifted in redshift by a small factor in order to improve the visualization only), which results in considerably more residual redshift variation. Note that the significantly higher q_{24} values for the Arp220-like *k*-correction results from the upturn in the Arp220-like correction at $z < 0.3$ and due to the particularly extreme silicate absorption features (cf. Fig. 1).

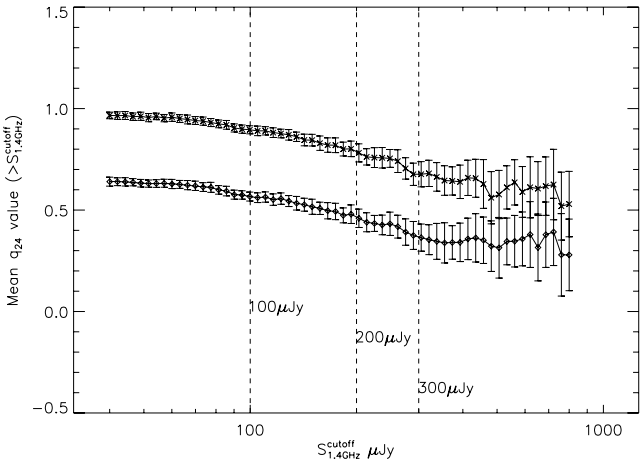

Figure 4. Mean q_{24} value as a function of cut-off in radio-flux density. Diamonds and crosses are based on the observed and M82-like *k*-corrected data, respectively, both showing similar dependencies with the cut-off in radio. The error bars represent the uncertainty on the mean value estimated using boot-strap resample technique. The vertical dashed lines are at 100, 200 and 300 μJy. Since sources with $S_{1.4\,\mathrm{GHz}} > 3.2$ mJy ($10^{-2.5}$ Jy) are essentially all radio-loud AGN (Condon 1984), these were not included in the estimation for the mean value.

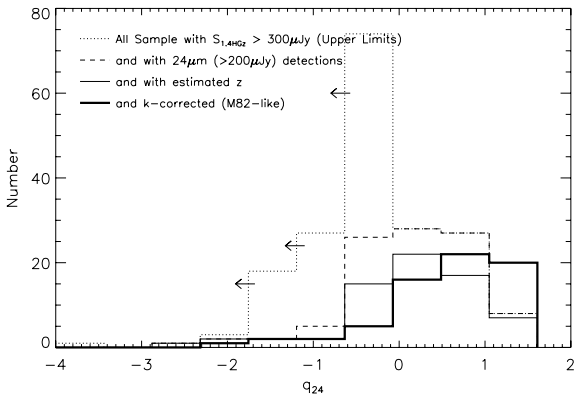

Figure 5. Histogram of the q_{24} values for the radio sources with radio-flux densities brighter than 300 μJy using different selection criteria. Upper limits are assumed considering $S_{24\,\mu\mathrm{m}} = 200$ μJy. The distribution for the *k*-corrected data using a M82-like template is plotted by a thick black line.

sources between $1 < z < 2$, we suggest no strong mid-IR-silicate absorption for the bulk of the sources.

The M82-like *k*-correction to all sources with detections at 24 μm in the range $0 < z < 1$ gives $q_{24} = 1.03 \pm 0.31$, in agreement with previous Appleton et al. (2004) estimation ($q_{24} = 1.00 \pm 0.27$). A simple linear regression to the M82-like *k*-corrected data is given by $q_{24}(z) = (0.94 \pm 0.01) + (-0.01 \pm 0.01)\,z$, suggesting a constant dependency (at 1σ level) for the q_{24} fraction with redshift. This result assumes that all galaxies in the sample can be fitted with a single M82-like template, although the fact that the correlation naturally appears to have the same mean and scatter as a function of redshift, up to $z \sim 3.5$, is highly suggestive that the FIR/radio correlation holds all the way back to primordial times.

3.3 The correlation based on a complete radio sample at 24 μm

The mean and scatter values quoted for the correlations described above may be being biased by incompleteness at 24 μm for sources with faint radio fluxes: a large number of star-forming-dominated radio sources with $S_{1.4\,\mathrm{GHz}} \lesssim 300$ μJy are not expected to have been detected at 24 μm. To demonstrate this problem, we plot in Fig. 4 the mean q_{24} as a function of a cut-off in the 1.4-GHz flux density. It clearly shows a decreasing trend for the mean q_{24} from fainter radio fluxes up to $S_{1.4\,\mathrm{GHz}} \approx 300$ μJy, where a flattening starts to appear. This means that considering a high enough radio cut-off, the correlation becomes independent of the radio sample. We, therefore, base the correlation on a complete radio sample by constraining the number of sources to those with $S_{1.4\,\mathrm{GHz}} > 300$ μJy. This radio sample is essentially complete at 24 μm for star-forming galaxies, and all residual 24-μm non-detections are associated with radio-loud AGN activity (see below).

Using the biweight estimator, we find that for the radio population with $S_{1.4\,\mathrm{GHz}} > 300$ μJy and mid-IR detections ($S_{24\,\mu\mathrm{m}} > 200$ μJy), the observed q_{24} values have significantly lower mean and larger scatter for the (non-*k*-corrected) correlation $q_{24} = 0.30 \pm 0.56$ (it changes to $q_{24} = 0.70 \pm 0.63$ for the subsample of sources at $0 < z < 1$).

A histogram of q_{24} for the sources with $S_{1.4\,\mathrm{GHz}} > 300$ μJy is shown in Fig. 5. It shows that the bulk of the undetected sources is found below $q_{24} = -0.18$ due to the 200-μJy threshold adopted for the mid-IR image. This value of q_{24} implies sources three times brighter in radio luminosity than those from our observed mean value $\langle q_{24}\rangle = 0.30$, and ∼10.5 times brighter than the observed mean value found by Appleton et al. (2004), $\langle q_{24}\rangle = 0.84$. Yun, Reddy & Condon (2001) have defined radio-excess sources as those whose radio luminosity is $\geqslant$5 times the value predicted from the FIR/radio correlation. In this sense, radio-loud AGN based on 24-μm detections are sensitive to the assumed mean value for the FIR/radio correlation (Appleton et al. 2004; Donley et al. 2005; Boyle et al. 2007). We find that 62 per cent of the radio sources (24 detections and 82 upper limits) plotted in Fig. 5 have $q_{24} < -0.18$. These values clearly suggest a large number of radio-loud AGN in this radio-flux regime.

It is worth noting that the incompleteness produced by sources without photometric redshifts (compare thick continuum and dashed lines in Fig. 5) does not introduce significant changes in the mean and scatter of the q_{24} distribution.

The *k*-corrected mean and scatter values (biweight estimator) for the distribution of sources with $S_{1.4\,\mathrm{GHz}} > 300$ μJy, mid-IR detections (>200 μJy) and estimated redshifts, change to

$q_{24} = 0.71 \pm 0.47, 1.25 \pm 0.47$ and 0.77 ± 0.48 after using the M82-like, Arp 220-like and Lagache et al. model, respectively. The bottom panel in Fig. 2 shows the M82-like k-corrected q_{24} values as a function of redshift for this subsample. It suggests a slight descending trend, from $z < 0.5$ to higher redshifts, probably associated with the presence of steeper mid-IR spectra for brighter radio sources, although it is not possible to statistically discriminate a better representative SED between the tested templates.

A simple linear regression to the M82-like k-corrected q_{24} distribution, based on radio sources brighter than 300 μJy and detected at 24 μm, is given by $q_{24}(z) = (0.71 \pm 0.04) + (-0.03 \pm 0.03)\,z$. For this complete radio sample, we also find a flat distribution at 1σ level, suggesting the validity of the FIR/radio correlation up to $z \approx 3.5$. Note, however, that even at these bright radio-flux densities, at $z \gtrsim 1$ the upper limits may overlap with the mean value found for the correlation, suggesting the possibility of confusion at higher redshifts between radio-loud AGN and those affected by mid-IR features in the SEDs. Future studies with submm and FIR facilities, such as SCUBA-2 and the *Herschel Space Observatory*, will help to better estimate the total bolometric FIR luminosity, and therefore discriminate between those sources affected by SED features or due to powerful radio AGN activity.

4 RADIO-LOUD AGN ACTIVITY

4.1 The transition form radio-loud AGN to star-forming-dominated galaxies

Making use of the M82-like k-corrected data presented in the last section, we have worked out a method of selecting radio-loud AGN from our radio sample, based on different q_{24} thresholds.

It is well known that most powerful radio sources (>1 mJy) are radio-loud AGN (Condon 1992), but the number counts obtained from deep radio surveys have suggested the appearance of a new, dominant population at fainter radio-flux densities. It is well established that this faint radio population may be composed of star-forming galaxies (Condon 1984) and radio-quiet AGN (Jarvis & Rawlings 2004). However, the transition from radio-loud AGN to star-forming galaxies is still not well defined.

To look at the relative fractions of these populations as a function of radio-flux density, we use the previous M82-like k-corrected data to identify radio-loud AGN based on different q_{24} cut-off thresholds (Donley et al. 2005). The main assumptions for the following results are the mean and scatter of the 24 μm/1.4 GHz correlation (Section 3.3), and the flux thresholds from the radio and mid-IR maps.

Fig. 6 shows three different diagrams for the expected fraction of starburst/radio-quiet AGN ('star-forming-dominated' systems [2]) and radio-loud AGN as a function of the 1.4-GHz flux density. A value of $q_{24} = \langle q_{24}\rangle - 2\sigma_{q_{24}}$ (i.e. 2σ below the mean value) is adopted as the cut-off value of q_{24} used to separate and distinguish 'star-forming-dominated' sources from radio-loud AGN. In particular, the cut-off used in the main panel of Fig. 6 is at $q_{24} = -0.23$, which

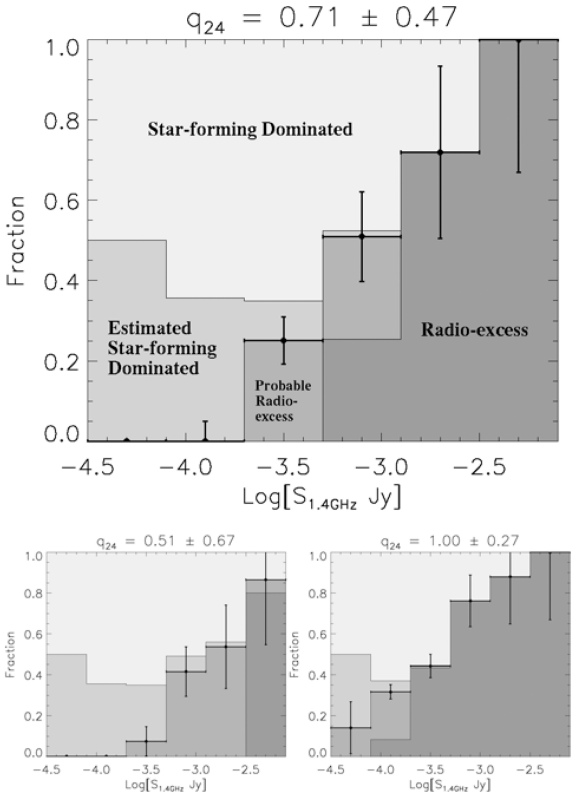

Figure 6. The submJy radio-flux transition from radio-excess sources to starburst-dominated sources based on different q_{24} thresholds using the M82-like k-corrected data. Sources without redshift have been included using a mean M82-like k-correction (+0.33), non-varying considerable the results but improving error bars. The 'radio-excess' fraction is composed of those sources detected at 24 μm, or with upper limits, with q_{24} less than 2σ from the mean value of the correlation. The 'star-forming-dominated' fraction is, therefore, that with q_{24} values above the 2σ threshold for radio-excess selection. The 'Probable star-forming-dominated' fraction is based on an estimation which corrects the incompleteness at 24 μm of the 'star-forming-dominated' sources (see the text for details). Hence, all the rest of the sources are very unlikely to follow the 24 μm/1.4 GHz correlation and are called the 'probable radio-excess' fraction. Error bars, based on the number counts, are 1σ confidence limits given by Gehrels (1986). The main upper panel shows our best estimate of the different populations, based on the results from Section 3.3. The small panels at the bottom consider the same grey-colour criteria. On the left-hand side, we modify the q_{24} mean and scatter based on the higher end of the correlation ($\langle q_{24}\rangle + \sigma_{q_{24}} \approx 1.2$), and on the right-hand side we use the previous Appleton et al. (2004) results.

in terms of luminosity means that radio-loud AGN are selected by having a radio power approximately nine times or larger than that predicted by the mean value. All radio sources with measured 24-μm flux densities and q_{24} values above the threshold are indicated in Fig. 6 as 'star-forming dominated'. The so-called 'radio-excess' fraction corresponds to all those sources detected at 24 μm with q_{24} below the cut-off value, or undetected but with upper limits below the threshold. The remaining population of sources will be those that are undetected at 24 μm but have upper limits in q_{24} that lie above the q_{24} threshold for AGN selection. Those will be a mixture of starburst/radio-quiet systems and radio-loud AGN.

We have already said in Section 3 that the faint radio population ($\lesssim$300 μJy) is affected by incompleteness at 24 μm. In fact, for sources that follow the FIR/radio correlation then, using the threshold for detection in the SWIRE data, we can predict the expected

[2] The reason we call these objects as star-forming-dominated sources comes only from the fact that they follow the FIR/radio correlation. Although, this is not entirely true because the radio emission from radio-quiet AGN (luminous Seyferts; sources that have been found to follow the correlation) takes the form of jets and suffers the same orientation-dependent beaming effects as the radio-loud AGN, implying it is most definitely AGN-related synchrotron emission.

fraction of detections at 24 μm as a function of radio-flux density. We can then use this to correct the observed fraction of star-forming sources for incompleteness. In order to do so, we ran Monte Carlo simulations for each radio-flux density bin (from Fig. 6), using the mean and scatter of the 24 μm/1.4 GHz correlation, to obtain the probability of detection based on the 24-μm image threshold at 200 μJy. The correction for incompleteness to the 'star-forming-dominated' population is called, in Fig. 6, the 'Estimated star-forming-dominated' fraction, which is mainly introduced at faint radio fluxes. The reminder of the uncertain population is classified as the 'probable radio-excess' fraction.

The main panel of Fig. 6 shows our best prediction for the transition from radio-loud-AGN- to a star-forming-dominated population at submJy radio fluxes. It makes use of the mean and scatter of the M82-like *k*-corrected q_{24} values (from Section 3.3) to define the threshold value and the inputs to the Monte Carlo simulations. It is found that for star-forming sources with $S_{1.4\,\mathrm{GHz}} = 200$–$500$ μJy ($10^{-3.7}$–$10^{-3.3}$ Jy), or with higher radio fluxes, the expected fraction of counterparts at 24 μm start to become complete. Actually, the Monte Carlo estimation predicts that $\gtrsim$85 per cent of the sources should have counterparts at 24 μm in this bin [it changes to $\gtrsim$98 per cent considering the Appleton et al. (2004) q_{24} values]. This confirms the previous estimation for the complete star-forming radio sample based on a cut-off at $S_{1.4\,\mathrm{GHz}} = 300$ μJy.

In order to show how the results change with uncertainties in the FIR/radio correlation, the two small panels at the bottom in Fig. 6 use an exaggerated scattering for the correlation, and the Appleton et al. (2004) result (left- and right-hand side, respectively), as indicated by the values above the panels. Each case, however, keeps almost the same fit to the high end of the q_{24} distribution ($\langle q_{24}\rangle + \sigma_{q_{24}} \approx 1.2$).

From our best fit, we predict a significant (25 ± 5 per cent) fraction of radio-loud AGN at flux levels of $S_{1.4\,\mathrm{GHz}} \sim 300$ μJy. The number of radio-loud AGN clearly increases as a function of the radio-flux density and above $S_{1.4\,\mathrm{GHz}} \gtrsim 3.2$ mJy ($10^{-2.5}$ Jy) essentially all radio sources are radio-loud AGN. At ∼50-μJy flux-density levels, the fraction of radio-loud AGN significantly decreases to zero ($\lesssim$20 per cent from the lower panel estimations), leaving the star-forming-dominated systems as the only population at this faint radio-flux regime.

These simple analyses suggest that a large number of radio-loud AGN could be selected using deep mid-IR and radio surveys based on a simple radio-excess selection criteria. In terms of the AGN population, we note that our predictions for the 'radio-excess' fraction are just part of the total number of AGN, because many radio-quiet AGN may be included in the 'star-forming-dominated' population.

4.2 Host galaxy properties

To explore the optical galaxy host properties of the different populations presented in Section 4.1, we estimated the rest-frame ($U - B$) colour (limited to sources with estimated redshift) for each source. The colour histograms for the three populations, 'star-forming-dominated' sources, the 'radio-excess' sources and 'All others' ('estimated radio excess' and 'estimated star-forming-dominated' fractions combined) are plotted in Fig. 7.

Considering only the population with radio-flux densities $S_{1.4\,\mathrm{GHz}} > 300$ μJy (left-hand panel), we find that both the 'radio excess' and 'All others' populations present clearly redder distributions compared to the 'star-forming-dominated' population. A Kolmogorov–Smirnov (KS) rejects the hypotheses that either the 'radio excess' or 'All others' sources are drawn from the same parent population as the 'star-forming-dominated' sources at >99.999 per cent significance in both cases, proving that they have a different nature. On the other hand, the colour distributions of the 'radio excess' and 'All others' populations are statistically indistinguishable. This similarity is expected because, as argued in Section 3.3, at these radio-flux densities the 'All others' population ought to be composed essentially entirely of 'radio-excess' sources (see Fig. 6). At lower radio-flux densities, the 'All others' population should contain a mixture of starburst-dominated galaxies and radio-loud AGN, and the right-hand panel of Fig. 7 shows that indeed at these lower fluxes this population has a more pronounced tail towards bluer $U - B$ colours.

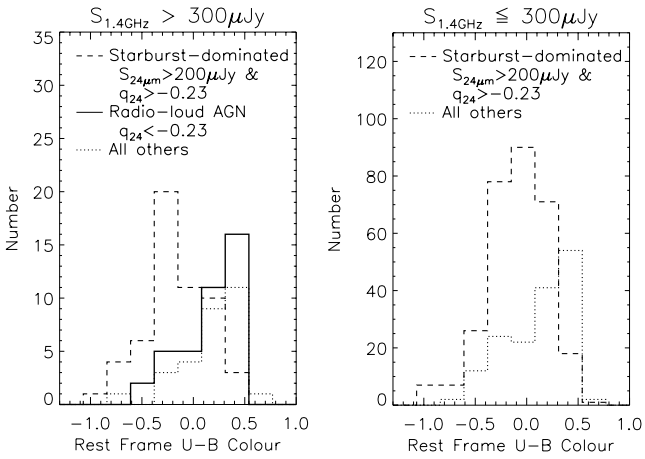

Figure 7. Histogram of rest-frame $U - B$ colours of all sources with estimated redshift in two bins of radio density flux. Dashed, continuum and dotted lines show the distribution of the 'star-forming dominated', 'radio excess' and 'All others' ('Estimated Star forming' and 'estimated radio excess') fractions, respectively. These correspond to the same ones plotted in the main panel of Fig. 6. It shows that the radio-excess population has a fundamentally different nature to the star-forming-dominated sources, and also confirms that at bright radio-flux densities (>300 μJy), the 'All Others' population is comprised almost entirely of radio-excess objects.

The red colours found for the radio-excess sources may come from the absence of star formation or due to dust obscuration in these sources. Since they do not have detections at 24 μm – probable absence of re-emission – we suggest that this radio-loud AGN population is hosted in red-galaxies with little or no star formation. This is potentially a very useful way to detect obscured AGN missed in deep X-Ray surveys, which are responsible of the bulk of the Cosmic X-Ray Background (Ueda et al. 2003).

5 DISCUSSION

Previous studies of the universality of the FIR/radio correlation at high redshift have combined 1.4-GHz data with *ISO* 15-μm data (Garrett 2002) and *Spitzer* 24- and 70-μm data (Appleton et al. 2004), both showing evidence of a correlation up to $z \sim 1$. More recently, Kovács et al. (2006) and Beelen et al. (2006) have shown evidence for the correlation at higher redshifts, for a sample of 15 submm galaxies ($z \sim 0.5$–3.5) and for a handful of distant quasars ($z \sim 2$–6), respectively. In this work, despite the difficulty of measuring a reliable bolometric FIR emission, the monochromatic 24-μm flux densities show a tight correlation with the 1.4-GHz flux density up to $z \approx 3.5$. *k*-corrections based on an M82-like template indicate that both the mean and the scatter of the q_{24} values remain constant as a function of redshift (see Fig. 3).

Table 1. Summary of the results presented in Section 3. The linear regressions are based on the detected sources at 1.4 GHz and 24 μm, using intrinsic error bars from the source extraction processes.

	Radio sample	q_{24} correlation mean and scatter	Linear regression	M82-like k-corrected q_{24} mean and scatter	Linear regression for the M82-like k-corrected q_{24}'s
(1)	$S_{24\,\mu m} > 200$ μJy	0.66 ± 0.39	$q_{24} = (0.85 \pm 0.01) - (0.20 \pm 0.01)\,z$	0.99 ± 0.32	$q_{24} = (0.94 \pm 0.01) - (0.01 \pm 0.01)\,z$
(2)	$S_{24\,\mu m} > 200$ μJy & $0 < z < 1$	0.80 ± 0.28		1.03 ± 0.31	
(3)	$S_{1.4\,GHz} > 300$ μJy & $S_{24\,\mu m} > 200$ μJy	0.30 ± 0.56	$q_{24} = (0.66 \pm 0.04) - (0.28 \pm 0.03)\,z$	0.71 ± 0.47	$q_{24} = (0.71 \pm 0.04) - (0.03 \pm 0.03)\,z$
(4)	$S_{1.4\,GHz} > 300$ μJy & $S_{24\,\mu m} > 200$ μJy & $0 < z < 1$	0.70 ± 0.63		0.95 ± 0.56	

The mean and scatter of the distribution of q_{24} values obtained after a M82-like k-correction for all radio sources detected at 24 μm is $q_{24} = 0.99 \pm 0.32$. This is in broad agreement with the results of Appleton et al. (2004), $q_{24} = 0.84 \pm 0.28$, based on a sample $z \lesssim 1$. However, if our sample is restricted to brighter radio sources for which all star-forming sources would be expected to have been detected at 24 μm, then the mean relation becomes $q_{24} = 0.71 \pm 0.47$, with a scatter about twice that of Appleton et al. The median error value for the q_{24}'s has been found to be about 0.1 dex, which suggests that this scatter is intrinsic for the correlation and does not come from observational errors. We can conceive of two possible explanations for this increased scatter at higher radio-flux densities. First, it may be that, because of the smaller number of sources, some radio-excess objects may fail to be excluded by the biweight estimator, and therefore both bias and increase the scatter of the relation. Secondly, it may be that for these more powerful sources, the M82-like template (a relatively low-luminosity source) is not an accurate representation of the FIR emission of all sources, but that a broader range of SED types is present, increasing the scatter. Fig. 2 provides some evidence for this: although a very flat q_{24} distribution is found in the full radio sample (top panel), some redshift variation may be present in the brighter radio sources (lower panel), in particular, the presence of a handful of sources with higher q_{24} values at low redshifts $z < 0.5$, which would be more consistent with a steeper mid-IR slope, such as that given by the Arp220-like template.

Recently, Boyle et al. (2007) have found a significantly higher mean value, $q_{24} = 1.39 \pm 0.02$ (2σ away from our estimation) whilst applying stacking techniques (Wals et al. 2005) to Australia Telescope Compact Array (ATCA) 1.4-GHz images using positions from *Spitzer* detections in the *Chandra* Deep Field South (CDFS) and European Large-Area ISO Survey (ELAIS) fields. Their work lacks redshift information, however, and therefore does not include k-corrections. We have shown the relevance of different mid-IR features for high-redshift sources at the flux regimes of this work, suggesting a clear underestimation for the intrinsic 24 μm/1.4-GHz scatter in their work. Also, a stacking analysis for a mixture of star-forming galaxies and radio-loud AGN does not discriminate an exclusive correlation for star-forming galaxies. Since the flux thresholds from our work are similar to their ones, we suggest that selection effects based on different sample selection criteria (from radio or mid-IR detections) may also be affecting the scatter on the 24 μm/1.4-GHz correlation.

The FIR/radio correlation in not precisely linear, specially in optically selected samples containing faint galaxies. It is expected that the radio emission, in low-luminosity galaxies, is more deficient since cosmic rays are more likely to escape from the galaxy (Chi & Wolfendale 1990). At redshifts larger than unity the Cosmic Microwave Background might quench the radio emission (Condon 1992) and cosmic evolution for the magnetic fields cannot be rejected either. Nevertheless, in this work, the exploration of more detailed models, showing for example luminosity (or mass) dependencies for the q_{24} parameter, was limited by the uncertainties in photometric redshifts.

A simple radio-flux estimation ($S^{\rm limit}_{1.4\,GHz} \approx 35$ μJy) shows that a starburst galaxy with a typical M82 luminosity can be observed up to moderate redshifts only, $z \sim 0.4$. In fact, it is expected that the observed high-redshift high-luminosity Universe is composed mainly of ULIRGs and AGN. ULIRGs are usually related to interacting systems (Sanders et al. 1988) and are expected to suffer strong absorption, implying large k-corrections for the 24-μm emission. Insights for steeper mid-IR SED at $S_{1.4\,GHz} > 300$ μJy are hinted (Fig. 2, bottom panel); however, the lack of a clear scatter excess in the FIR/radio distribution at $z \approx 1$–2 (Fig. 1) suggests that the bulk of the ULIRG-like high-redshift sources from our sample do not suffer large variations due to silicate absorption. The correlation found in this work is therefore quite unexpected, but suggests that a M82-like mid-IR template, intrinsically coming from a lower luminosity source, is still a good representation for the mid-IR SED of high-redshift star-forming-dominated systems. The M82-like template is also supported by Lagache's ULIRG ($L_{\rm IR} = 10^{12}\,{\rm M}_{\odot}$) model, and particularly leaves Arp 220 as single extreme case. These results are more relevant considering that Kasliwal et al. (2005) estimate that about half of ULIRGs at $z \approx 1$–1.8 may be unobserved at 24 μm due to silicate absorption at 9.7 μm in the Bootes field, a suggestion not particularly supported by our data. For ULIRGs selected in submm observations, their mid-IR SED is still under debate, but templates such as M82 and Arp 220 (Menéndez-Delmestre et al. 2007; Pope et al. 2006, respectively) have been found as good fits for their mid-IR range.

In Section 4, we have shown the capabilities of deep mid-IR and radio imaging for the selection of radio-loud AGN ('radio excess') based on different cut-offs in q_{24}. We have shown that at $S_{1.4\,GHz} > 300$ μJy, selected radio-excess sources strongly suggest nuclear activity. The radio-excess sources present a redder distribution of rest-frame $U - B$ colours compared with those identified as star-forming-dominated galaxies. This strongly suggests a different nature between the populations selected by the simple q_{24} threshold at -0.23. Previous population synthesis models (Jarvis & Rawlings 2004) have predicted that radio-excess sources at these flux densities are mainly FR type I (Fanaroff & Riley 1974). It is known that FR type I do not fall into the standard unified scheme for AGN (Antonucci 1993) and show no bright AGN nucleus. Therefore, their red colours indicate that these radio-loud sources do not present

significant star-formation activity and/or are hosted in red massive galaxies.

Jarvis & Rawlings (2004) predict that approximately half of the sources with radio fluxes between $100\,\mu\mathrm{Jy} \leqslant S_{1.4\,\mathrm{GHz}} < 300\,\mu\mathrm{Jy}$ present radio-loud activity. We have predicted from our best fit a fraction of 25 ± 5 per cent at this flux regime, in disagreement by a factor of 2 with their estimation. Fig. 6 shows that Appleton et al. estimation may explain a 50 per cent fraction, although we demonstrated in Section 3.3 that incompleteness biases the assumptions of those results. On the other hand, Simpson et al. (2006) tentatively suggested a radio-quiet AGN fraction of 20 per cent at this radio fluxes regime, but since radio-quiet sources have been found to also follow the FIR/radio correlation, in this work we are not able to discriminate between this population and starburst galaxies. Therefore, this radio-quiet AGN population remains uncertain.

6 CONCLUSIONS

We have analysed the 24-μm properties of a radio-selected sample in order to explore the well-known FIR/radio correlation at high redshifts. We have shown evidence that 24-μm data do not give the best estimation of the total bolometric FIR emission, reflected in a considerably larger scatter on the correlation than previous work using longer wavelengths (IRAS/60 μm – Yun et al. 2001, *Spitzer*/70 μm – Appleton et al. 2004). Nevertheless, despite the large scatter, the IR-24 μm/radio-1.4 GHz correlation seems to extend up to redshift $\sim$3.5 with roughly the same mean and scatter. The fact that we do not observe considerable variations in the correlation as a function of redshift, mainly seen on the well-defined upper end of the k-corrected q_{24} distribution (see top panels, Figs 2 and 3), highly suggests its validity all the way back to primeval times. This is the first evidence for the extension of the correlation over this very wide range of redshifts.

Statistically, the correlation is described by the basic observable parameter q_{24}, the ratio between the flux densities at 24 μm and 1.4 GHz, respectively. The q_{24} factor parametrize the link (in the local Universe at least) that star-forming galaxies have between the synchrotron emission, from cosmic rays accelerated by massive supernovae explosions, i.e. the massive end of the mass function in galaxies, with the reprocessed UV photons re-emitted by the dust at FIR wavelengths. Besides an intrinsic scatter for the correlation, the presence of an AGN may also modify the mid-IR spectra and the radio emission, biasing, and therefore increasing the scatter on a q_{24}-based correlation. We found a mean value (biweight estimator) of $q_{24} = 0.30 \pm 0.56$ for the observed and $q_{24} = 0.71 \pm 0.47$ for the k-corrected (M82-like) data based on an expected complete radio sample ($S_{1.4\,\mathrm{GHz}} > 300\,\mu\mathrm{Jy}$) at 24 μm.

Three different k-corrections has been tested: two based on well-known local starburst sources (M82 and Arp 220) and one on a SED ULIRG model (Lagache et al. 2004). The main difference introduced by using different templates is caused by the silicate absorption feature at $\sim$10 μm being redshifted into the observed 24-μm band at $z \approx 1$–2 (Fig. 1). Based on the smallest scatter found for q_{24} data, we propose an acceptable k-correction given by an M82-like mid-IR template, which suggests no strong evidence for extreme silicate absorption in the bulk of our sample. We do, however, find tentative evidence for a steeper mid-IR spectrum than M82 for brighter radio sources $>300\,\mu\mathrm{Jy}$, in order to explain the slight offset from the correlation for sources with $z < 0.5$.

We have found a clear dependency for the detected number of star-forming-dominated galaxies (starburst and radio-quiet AGN) as a function of the radio-flux density. Making use of the derived 24 μm/1.4 GHz correlation, and the flux density threshold from the 24-μm image, we ran Monte Carlo simulations to estimate the incompleteness at 24 μm, and therefore the intrinsic fraction of star-forming-dominated galaxies. This allowed us to estimate the probable number of radio-loud AGN and to describe the transition from AGN- to star-forming-dominated galaxies at faint radio-flux densities ($\lesssim$1 mJy). Our best-fitting estimation predicts a significant fraction (25 ± 5 per cent) of radio-loud AGN at $S_{1.4\,\mathrm{GHz}} \sim 300\,\mu\mathrm{Jy}$, rising quickly to become a dominant AGN population at brighter radio-flux densities (>1 mJy), and falling towards zero (certainly $\lesssim$20 per cent) at fainter fluxes. These results are in broad agreement with previous studies (e.g. Condon 1984).

We have also shown that the rest-frame $U - B$ colours, of the sources that are expected to be radio-loud AGN, have a redder distribution than the starburst/radio-quiet AGN galaxies (Fig. 7), strongly suggesting a different nature between the sources selected by our simple $q_{24} = -0.23$ threshold. These radio-excess sources seem to be hosted in red galaxies with little or no star-formation implied by the non-detection at 24 μm. This is therefore an extremely promising way to select obscured type 2 AGN (Comastri et al. 1995), with a radio-loud nature, which are missed by deep X-ray observations. Nevertheless, future spectroscopic follow-up of these sources, and also a better description of the FIR emission, is needed to fully test this method.

ACKNOWLEDGMENTS

This paper was supported by a Gemini–STFC research studentship. EI thanks to A. Pope, G. Lagache, P. Lira and B. Brandl for templates and useful comments to the paper. PNB, RM, IRS and OA acknowledge support from the Royal Society.

REFERENCES

Antonucci R., 1993, ARA&A, 31, 473
Appleton P. N. et al., 2004, ApJS, 154, 147
Beelen A., Cox P., Benford D. J., Dowell C. D., Kovács A., Bertoldi F., Omont A., Carilli C. L., 2006, ApJ, 642, 694
Beers T. C., Flynn K., Gebhardt K., 1990, AJ, 100, 32
Boyle B. J., Cornwell T. J., Middelberg E., Norris R. P., Appleton P. N., Smail I., 2007, MNRAS, 376, 1182
Brandl B. R. et al., 2006, ApJ, 653, 1129
Bruzual G., Charlot S., 2003, MNRAS, 344, 1000
Carilli C. L., Yun M. S., 2000, ApJ, 530, 618
Chi X., Wolfendale A. W., 1990, MNRAS, 245, 101
Cirasuolo M. et al., 2007, MNRAS, 380, 585
Comastri A., Setti G., Zamorani G., Hasinger G., 1995, A&A, 296, 1
Condon J. J., 1984, ApJ, 287, 461
Condon J. J., 1992, ARA&A, 30, 575
Dale D. A., Helou G., Contursi A., Silbermann N. A., Kolhatkar S., 2001, ApJ, 549, 215
Donley J. L., Rieke G. H., Rigby J. R., Perez-Gonzalez P. G., 2004, BAAS, 36, 1390
Donley J. L., Rieke G. H., Rigby J. R., Pérez-González P. G., 2005, ApJ, 634, 169
Dunlop J. S., Peacock J. A., 1990, MNRAS, 247, 19
Dye S. et al., 2006, MNRAS, 372, 1227
Elvis M. et al., 1994, ApJS, 95, 1
Fanaroff B. L., Riley J. M., 1974, MNRAS, 167, 31P
Feigelson E. D., Nelson P. I., 1985, ApJ, 293, 192
Garn T., Green D. A., Hales S. E. G., Riley J. M., Alexander P., 2007, MNRAS, 376, 1251
Garrett M. A., 2002, A&A, 384, L19
Gehrels N., 1986, ApJ, 303, 336

Haarsma D. B., Partridge R. B., Windhorst R. A., Richards E. A., 2000, ApJ, 544, 641
Harwit M., Pacini F., 1975, ApJ, 200, L127
Helou G., Soifer B. T., Rowan-Robinson M., 1985, ApJ, 298, L7
Hogg D. W., Baldry I. K., Blanton M. R., Eisenstein D. J., 2002, preprint (astro-ph/0210394)
Holland W. et al., 2006, in Zmuidzinas J., Holland W. S., Withington S., Duncan W. D., eds, Proc. SPIE Vol. 6275, Millimeter and Submillimeter Detectors and Instrumentation for Astronomy III. SPIE, Bellingham, p. 45
Hughes D. H. et al., 1998, Nat, 394, 241
Ivison R. J. et al., 2007a, ApJ, 660, L77
Ivison R. J. et al., 2007b, MNRAS, 380, 199
Jarvis M. J., Rawlings S., 2004, New Astron. Rev., 48, 1173
Kasliwal M. M., Charmandaris V., Weedman D., Houck J. R., Le Floc'h E., Higdon S. J. U., Armus L., Teplitz H. I., 2005, ApJ, 634, L1
Kinney A. L., Calzetti D., Bohlin R. C., McQuade K., Storchi-Bergmann T., Schmitt H. R., 1996, ApJ, 467, 38
Kovács A., Chapman S. C., Dowell C. D., Blain A. W., Ivison R. J., Smail I., Phillips T. G., 2006, ApJ, 650, 592
Lagache G. et al., 2004, ApJS, 154, 112
Lawrence A. et al., 2007, MNRAS, 379, 1599
Lonsdale C. J. et al., 2003, PASP, 115, 897
Menéndez-Delmestre K. et al., 2007, ApJ, 655, L65
Mignoli M. et al., 2005, A&A, 437, 883
Miyazaki S. et al., 2002, PASJ, 54, 833
Poglitsch A. et al., 2006, 36th COSPAR Scientific Assembly, 36, 215
Pope A. et al., 2006, MNRAS, 370, 1185
Roy A. L., Norris R. P., Kesteven M. J., Troup E. R., Reynolds J. E., 1998, MNRAS, 301, 1019
Sanders D. B., Soifer B. T., Elias J. H., Neugebauer G., Matthews K., 1988, ApJ, 328, L35
Sekiguki K. et al., 2005, in Renzini A., Bender R., eds, Multiwavelength Mapping of Galaxy Formation and Evolution. Springer-Verlag, Berlin, p. 82
Shupe D. L. et al., 2008, AJ, 135, 1050
Silva L., Granato G. L., Bressan A., Danese L., 1998, ApJ, 509, 103
Simpson C. et al., 2006, MNRAS, 372, 741
Smail I., Ivison R. J., Blain A. W., 1997, ApJ, 490, L5
Spergel D. N. et al., 2007, ApJS, 170, 377
Surace et al., 2005, The Swire Data Release 2, August 31, 2005
Ueda Y., Akiyama M., Ohta K., Miyaji T., 2003, ApJ, 598, 886
van der Kruit P. C., 1971, A&A, 15, 110
Wals M., Boyle B. J., Croom S. M., Miller L., Smith R., Shanks T., Outram P., 2005, MNRAS, 360, 453
Warren S. J. et al., 2007, MNRAS, 375, 213
Windhorst R. A., Miley G. K., Owen F. N., Kron R. G., Koo D. C., 1985, ApJ, 289, 494
Yamada T. et al., 2005, ApJ, 634, 861
Yun M. S., Reddy N. A., Condon J. J., 2001, ApJ, 554, 803

This paper has been typeset from a TEX/LATEX file prepared by the author.